Supporting information

K^+ regulated vanadium oxide heterostructure enables high-performance aqueous Zinc-ion battery

Haibing Li [a], Liyun Zhu [a], Weijun Fan [a], Yi Xiao [b], Jiadong Wu [c], Hongyu Mi [d], Fumin Zhang [e], Linyu Yang [c*]*

[a] College of Modern Science and Technology, China Jiliang University, Jinhua 322000, PR China. E-mail: lihaibing18@mails.ucas.ac.cn;

[b] Division of International Cooperation, Science&Technology Department of Xinjiang Uygur Autonomous Region, Urumqi 830011, P.R. China.

[c] School of physics and technology, Xin Jiang University, Urumqi, Xinjiang 830046, China. E-mail: yanglinyu0222@sina.com.cn;

[d] School of Chemical Engineering and Technology, Xinjiang University, Urumqi 830046, China.

[e] State Key Laboratory of Precision Measurement Technology and Instruments, Tianjin University, Tianjin 300072, P.R. China.

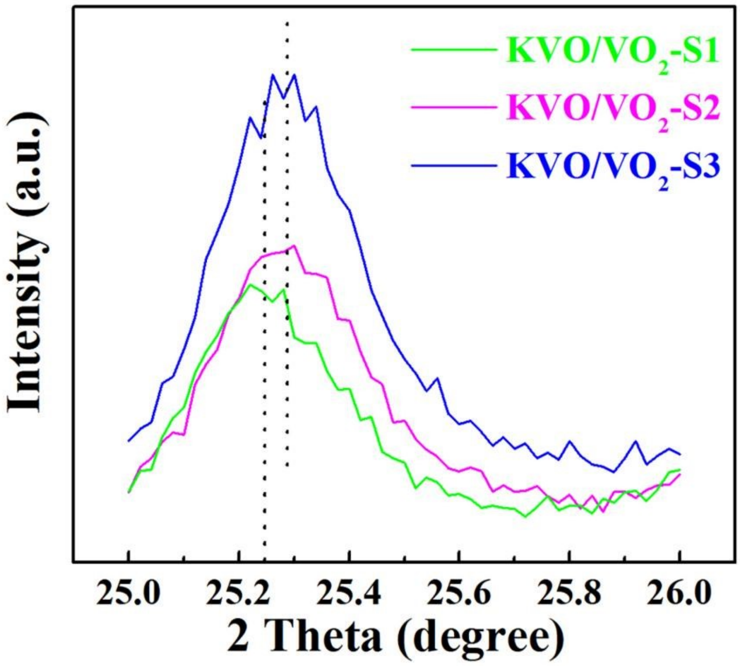

Fig. S1 Shifts of the diffraction peak of KVO/VO_2-S1, KVO/VO_2-S2 and KVO/VO_2-S3.

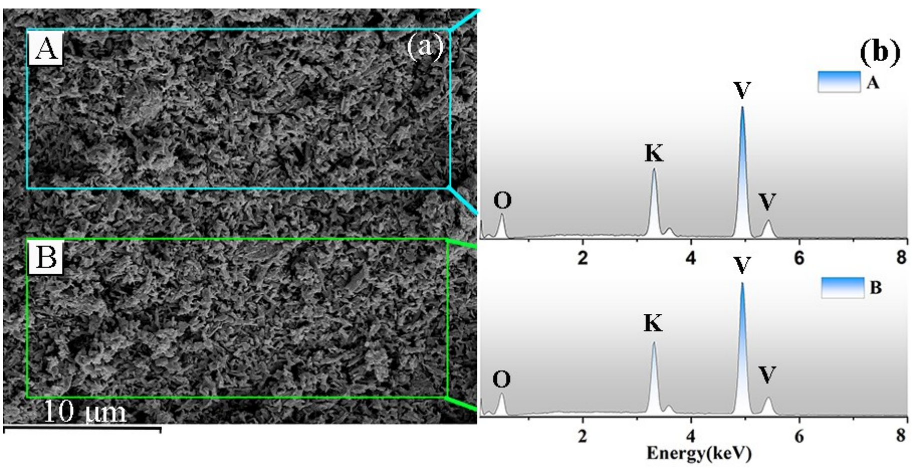

Fig. S2 SEM images and corresponding EDS spectra of KVO/VO_2-S2.

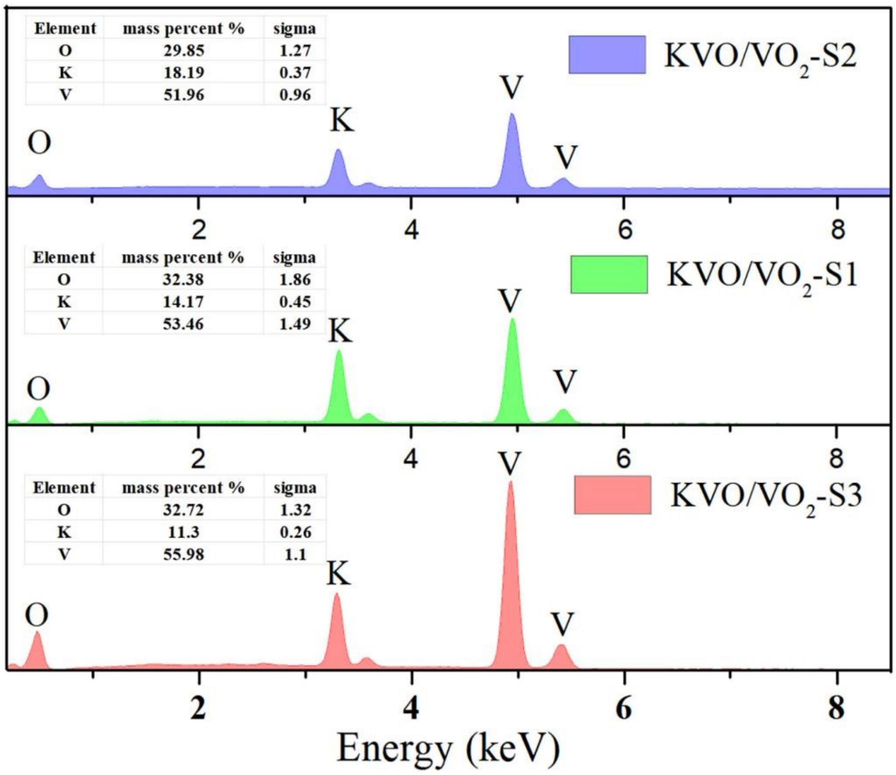

Fig. S3 EDS of the KVO/VO_2-S1, KVO/VO_2-S2 and KVO/VO_2-S3, respectively.

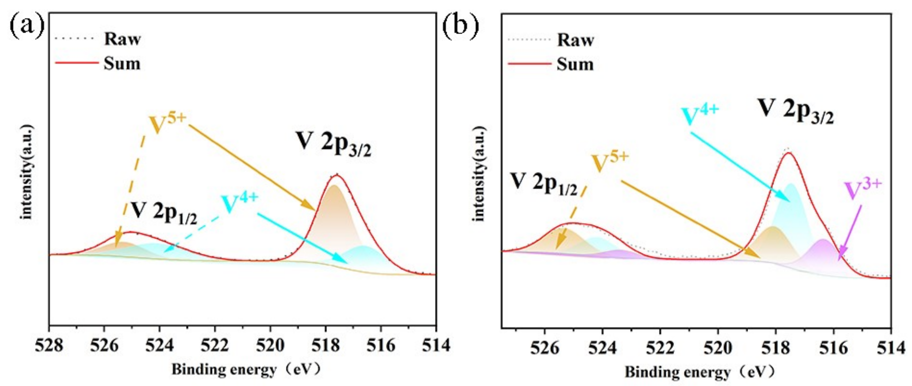

Fig. S4 High-resolution V 2p spectra of the KVO/VO_2-S1 and KVO/VO_2-S3 sample, respectively.

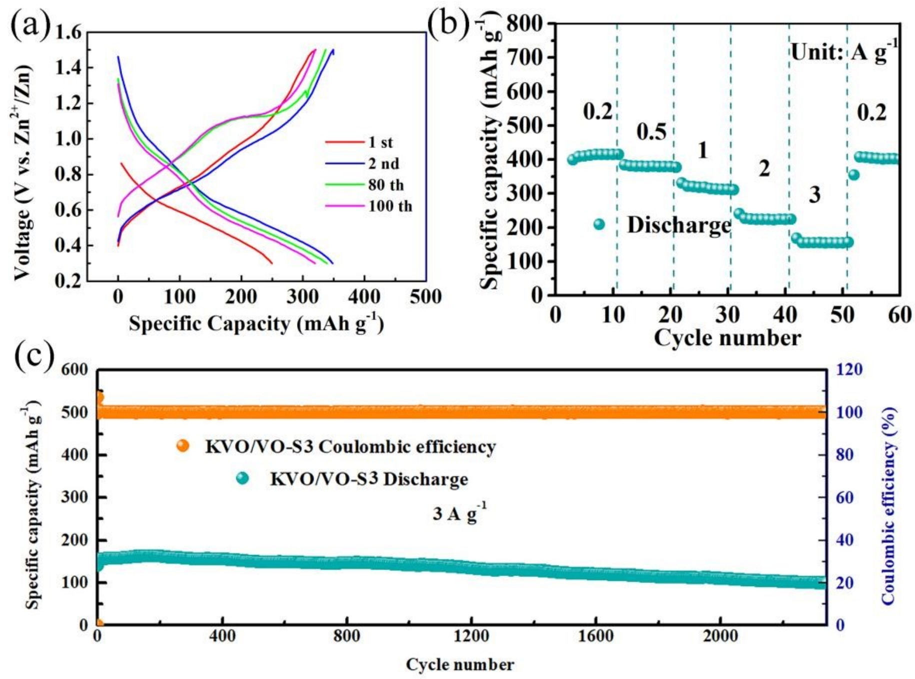

Fig. S5 (a) GCD profiles at current density of 0.2 A g^{-1}, (b) rate performance at different current density of 0.2, 0.5, 1, 2, 3 A g^{-1}, (c) long cyclic performance of KVO/VO_2-S3 at a current density of 3 A g^{-1}.

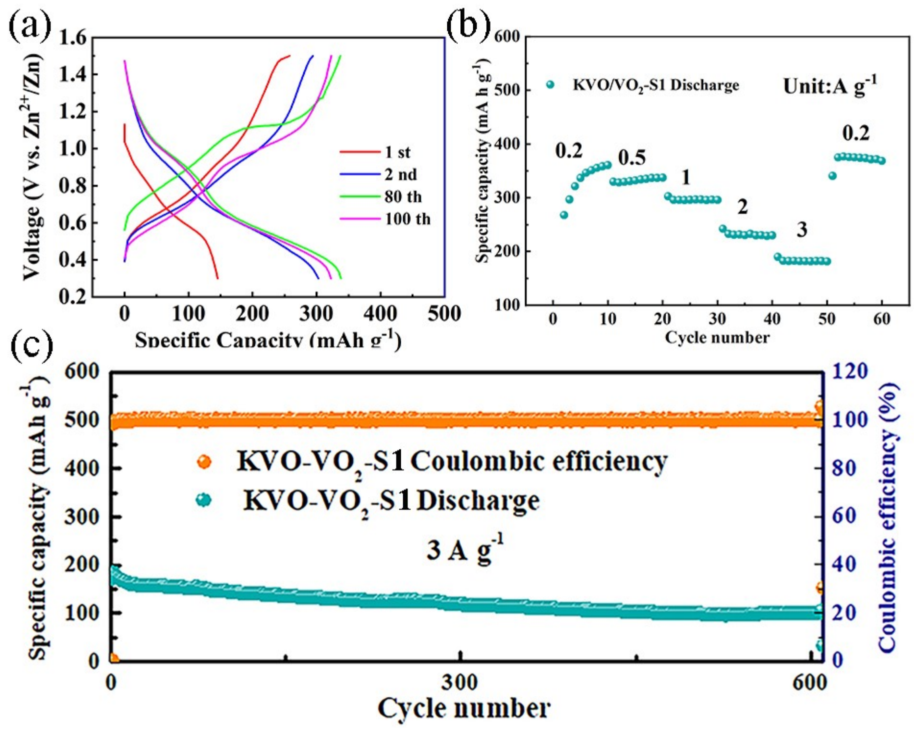

Fig. S6 (a) GCD profiles at current density of 0.2 A g^{-1}, (b) rate performance at different current density of 0.2, 0.5, 1, 2, 3 A g^{-1}, (c) long cyclic performance of KVO/VO_2-S1 at a current density of 3 A g^{-1}.

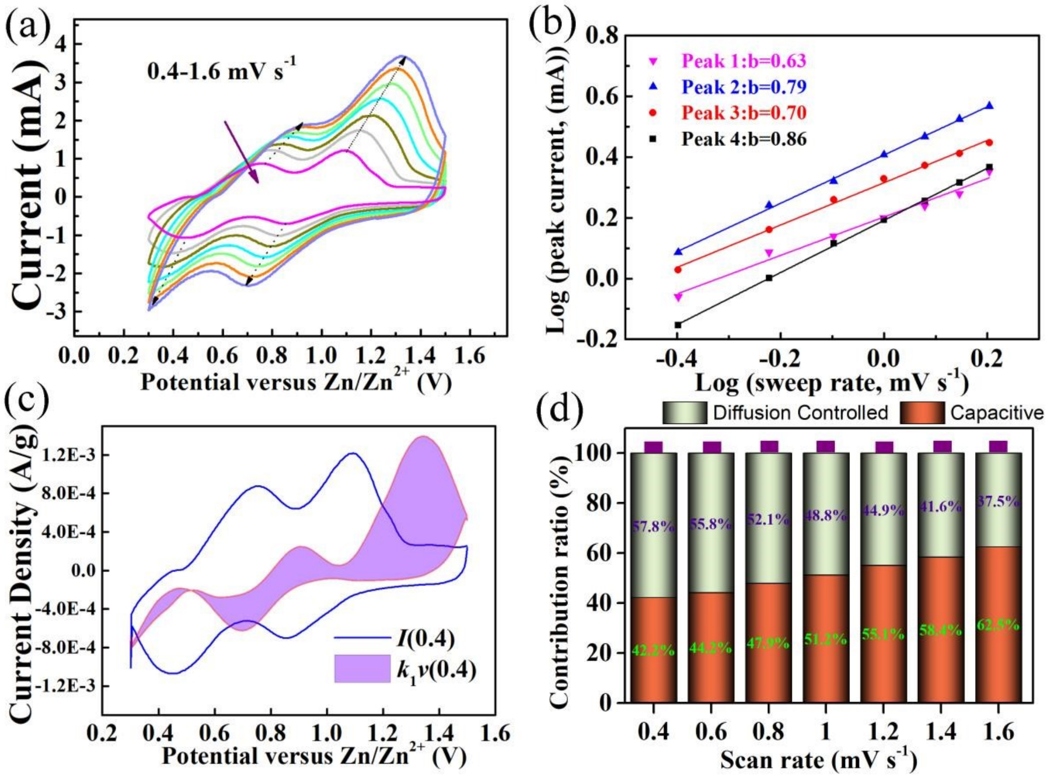

Fig. S7 (a) CV curves under different scan rate from 0.4-1.6 mV s^{-1}. (b) calculated b value by log(i) vs log(v) plot at special peak currents. (c) CV curve with the pseudocapacitive ratio presented by the shaded area at scan rate of 0.4 mV s^{-1}. (d) percents of surface–controlled capacities and diffusion–controlled capacities at a scan rate from 0.4 to 1.6 mV s^{-1} of KVO/VO_2-S3 cathode.

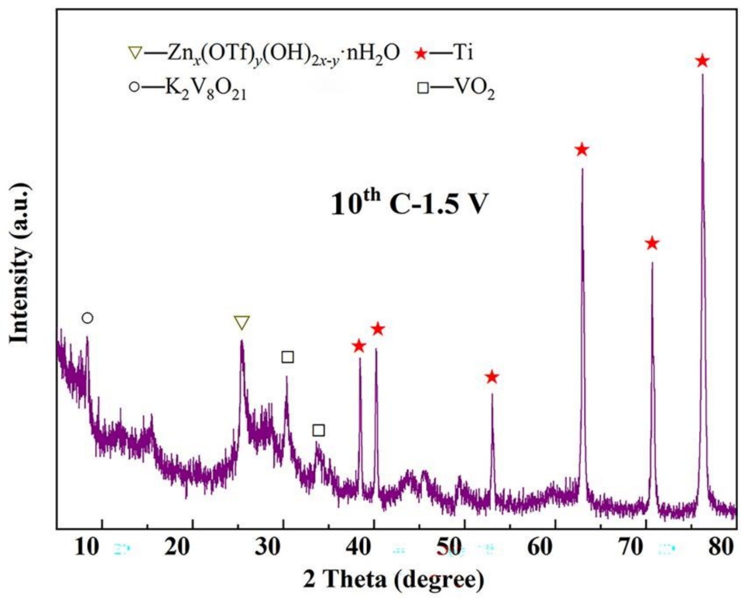

Fig. S8 The ex-situ XRD pattern of KVO/VO_2-S2 cathode at different charge/discharge states (pristine and 50th C-1.5V).

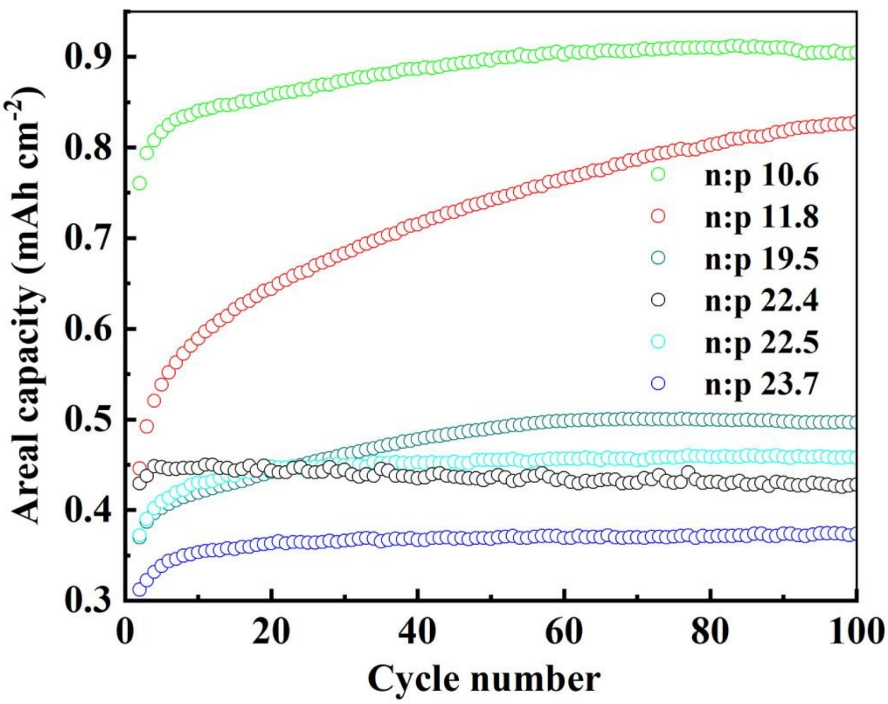

Fig. S9 Cyclic performance of KVO/VO_2-S2 cathode at different n/p ratios and areal current density.

Table S1. Performance of comparison.

Materials	Current density(A g^{-1})	Special capacity(mAh g^{-1})	Current density(A g^{-1})/cycle number	Capacity retention
V_2O_5 [18]	0.2	403	1/1000	70.4%
$K_2V_3O_8$ nanoflower [40]	0.1	302.8	4.0/2000	92.3
V_2O_5/V_2C heterostructure [34]	1.0	412.0	20/6000	53.2
V_2O_5/VO_2 heterostructure [41]	0.2	453.6	1.0/800	85.6
$Mn_xV_2O_6$+V_2C heterostructure [36]	0.1	437.0	2.0/1000	72%
$Mn_2V_2O_7$+V_2O_3 [42]	0.5	312.0	1.0/1000	87%
MnO_2+PVP [43]	0.125	317.2	10/20000	100%
$ZnNi_{0.5}MnO$/NCNTs [44]	0.1	239.2	1.0/3000	45%
$NaV_3O_8\cdot1.5H_2O$ [45]	0.1	334.4	1.0/3000	87%
$Zn_{0.52}V_2O_5$ [46]	0.2	286.2	20/18000	95.4%
PEO-LiV_3O_8 superlattice nanosheets [47]	0.1	438.1	10/3000	89.8%
$Ca_{0.67}V_8O_{20}\cdot3.5H_2O$ nanobelts [48]	0.1	466.0	5/2000	74%
F-doped $NH_4V_4O_{10}$ [27]	0.1	465.0	4/2000	88%
$Zn_3(OH)_2V_2O_7\cdot2H_2O/NH_4V_4O_{10}$ nanobelts [49]	0.5	337.0	10/4000	94%
Mg_2VO_4/VO_2 heterostructures [50]	0.3	393.6	0.3/1000	83.6%
δ-$K_{0.49}V_2O_5$ nanobelts [51]	0.2	361.0	5/2000	90.3%
Our work	0.2	460.6	3/2500	90.7%

Table S2. Performance of comparison of batteries with different n/p ratios.

Sample	Mass loading ($mg\ cm^{-2}$)	n/p ratio	Areal current density ($mA\ cm^{-2}$)	Areal capacity ($mAh\ cm^{-2}$)
KVO/VO_2-S2 cathode	2.33	19.5	7.0	0.5
	4.13	11.8	12.4	0.8
	6.40	10.6	19.2	0.9
	7.50	23.7	22.5	0.4
	8.32	22.4	25.0	0.4
	9.51	22.5	28.5	0.4